Malaysian Journal of Catalysis

MJCat

Stoichiometric effects of feed ratio on syngas production from CO₂ reforming of methane over SmCoO₃ perovskite catalyst

Osarieme Uyi Osazuwa and Chin Kui Cheng*

Faculty of Chemical & Natural Resources Engineering, Universiti Malaysia Pahang, Lebuhraya Tun Razak, 26300 Gambang Kuantan, Pahang, Malaysia,
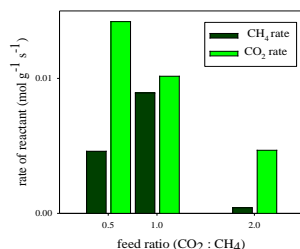**Corresponding Author: chinkui@ump.edu.my*

GRAPHICAL ABSTRACT

ABSTRACT

An effective way of consuming the two most dominant gases (CO_2 and CH_4) which are heavily linked with heat waves across the globe is the CO_2 reforming of methane reaction. This study describes the use of sol-gel citrate method to prepare $SmCoO_3$ perovskite catalyst and thereafter, catalytic test was carried out on the methane reforming reaction platform to produce syngas. The physicochemical properties of $SmCoO_3$ perovskite catalyst were determined pre-activity evaluation by TGA, N_2 physisorption, EDX, XRD, and post-activity evaluation by EDX and TGA. Results from the pre-reaction characterization showed the formation of crystalline and monophasic perovskite structure, while the post-reaction characterization showed evidence of carbon species associated with methane reforming reactions. The catalytic reaction was performed at atmospheric pressure on a reactor bed using a gas hourly space velocity of 30,000 h^{-1} and the activity was studied at stoichiometry (CO_2: CH_4 1:1), below (CO_2: CH_4 1:2) and above stoichiometry (CO_2: CH_4 2:1) of reactant gas at reaction temperature of 1023 K. Results showed highest CO_2 and CH_4 conversion of 85% and 84% respectively and optimum syngas yield (H_2: CO) of 60% and 57% respectively at stoichiometry ratio.

Keywords: Dry reforming, Methane, Perovskite, SmCoO₃, Syngas

1.   INTRODUCTION

The increasing demand for an alternate source of energy due to the fast depletion of fossil fuel has recently been attracting attention from researchers [1]. Hence, the utilization of methane and carbon dioxide which are the main greenhouse gases is on the increase. Reports show that methane reserves are much larger than crude oil reserves due to the fact that methane can be produced from various sources. Methane reforming is of three types; steam, partial oxidation and carbon dioxide reforming. This process produces synthesis gas which is an important feedstock for chemical production in industries and also the Fischer–Tropsch synthesis. Commercially, steam reforming of methane is a more attractive reforming technique equation (1) [1].

$$CH_4 + H_2O \rightarrow CO + 3H_2 \quad \Delta H_{298\,K} = 225.0 \text{ kJ mol}^{-1} \quad (1)$$

However, drawbacks to the steam reforming reaction include; high energy consumption, deficiency of CO, and its unsuitability for the Fischer–Tropsch synthesis. Catalytic partial oxidation of methane has also been studied equation (2) [2].

$$CH_4 + \frac{1}{2}O_2 \rightarrow CO + 2H_2 \quad \Delta H_{298\,K} = -22.6 \text{ kJ mol}^{-1} \quad (2)$$
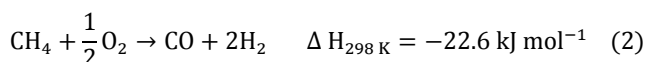
This process produces a much better ratio of syngas. Although due to the high temperature requirement of the reaction, the process becomes difficult to control [1]. The replacement of H_2O and O_2 by CO_2 yields a much lower H_2/CO ratio; approximately 1.0 in the product stream. This ratio is suitable for the effective utilization of synthesis gas. Also, with respect to the environment, the CO_2 reforming process is preferable due to the fact that it utilizes the emitted CO_2 and CH_4 gas thereby reducing global warming and minimizing the greenhouse effect equation (3) [3].

$$CH_4 + CO_2 \rightarrow 2CO + 2H_2 \quad \Delta H_{298\,K} = 247.0 \text{ kJ mol}^{-1} \quad (3)$$

Methane dry reforming is a catalytic reaction prone to catalyst deactivation due to carbon formed on the catalyst surface [4]. Developing a catalyst, which minimizes carbon formation on the catalyst surface, is highly desired. Noble metal based catalyst inhibits carbon formation better than Ni-based catalyst [5]. However, Ni-based catalyst is readily available and is more economical, [6].

Transition metal based catalyst have been reported to show good activity in methane dry reforming [7]. Incorporating the transition metal (Ni or Co) into the perovskite structure can also improve the catalyst performance. The catalytic nature of perovskite based catalyst (ABO₃) depends on the properties of *A* and *B* and their oxidation states. Component *A* and *B* are cations while *O* which is oxygen is an anion. Perovskite oxides possesses

very good redox properties, which promotes catalytic performance and minimizes carbon formation on the catalyst surface [8].

Therefore, the objective of this study is to synthesize, characterize, and determine the stoichiometric effects of feed gas in the methane dry reforming reaction using a perovskite catalyst ($SmCoO_3$). The catalyst was synthesized using the sol-gel citrate method, followed by characterization of the fresh catalyst. Catalytic activity test was carried out at stoichiometry, below and above stoichiometry to determine the effects reactants concentration on the conversion of the greenhouse (CO_2 and CH_4) gases and the formation of syngas (H_2 and CO).

2. EXPERIMENTS

2.1 Catalyst Preparation

Perovskite based catalyst; $SmCoO_3$ was synthesized by the sol-gel citrate method. This method has been used by several researchers in literature [9], [10]. The catalyst was prepared by the following procedure: A solution of citric acid was prepared and Co $(NO_3)_2.6H_2O$ was added. The solution was mixed until dissolved before Sm $(NO_3)_3.6H_2O$ was added to the solution. The solution was stirred for 4 h, while increasing the temperature from room temperature to 353 K. The gel obtained was dried at 383 K and calcined at 1123 K in a furnace with a ramping of 5 K min^{-1}. In the course of the preparation, the chelating agent to metallic ions ratio used was 2:1 respectively.

2.2. Characterization

The primary elemental composition and morphology of the fresh catalyst and the used catalyst was established using a HITACHI bench top EDX analyzer. X-ray diffraction (XRD) was performed with a RIGAKU miniflex II X-ray diffractometer from 3° to 80° in 2θ scanning range using monochromatized $CuK\alpha$ radiation with wavelength (λ) of 0.154 nm at rate of 0.02^o (2θ) and a counting speed of 1s. The crystallites size for $SmCoO_3$ was calculated from the XRD using the Debye-Scherrer equation equation (4) [11].

$$D_{hkl} = \frac{0.9\lambda}{\beta_{hkl}cos\theta} \quad (4)$$

Where the crystallites magnitude of the $SmCoO_3$ perovskite oxide is D_{hkl}, λ is the wavelength of Cu-K_α, β_{hkl} is the peak full width with half maximum and θ is the Bragg diffraction angle.

Adsorption-desorption isotherms were measured using a thermo scientific acquisition analyzer equipped with degasser station and surfer acquisition (version 1.2.1) software. BET surface area was determined by placing the sample in the BET cell, degassed under vacuum at 573 K and analyzed at 77 K.

Thermogravimetric analysis (TG) was carried out using TA instruments, Q 500 series to study the solid-state phase change and carbon deposition. Temperature ranging from 298 to 1173 K and heating increments of 10 K min^{-1} was used in the presence of air.

2.3. Catalytic activity

100 mg of solid $SmCoO_3$ perovskite catalyst was tested in a 10-mm ID stainless steel tubular reactor supported by quartz wool. Feed ratio ranging from 0.5 to 2.0 was employed at 1023 K under barometric condition. The total flow rate of feed gas was 50 ml min^{-1} STP, which peaks at a weight hourly space velocity of 30,000 ml g^{-1} h^{-1}. Product gas was collected and analyzed every hour for 8 h in order to ensure steady state condition. During all experimental run the $SmCoO_3$ perovskite catalyst was used without previous reduction as the catalyst showed great reducing tendencies during reaction.

A gas chromatography instrument (GC-Agilent 6890 N series) equipped with a thermal conductivity detector for detecting CO_2, CH_4, H_2 and CO was used to analyzer exit gas composition. Two packed columns; Supelco Molecular Sieve 13 × (10 ft × 1/8 in OD × 2 mm ID, 60/80 mesh, stainless steel) and Agilent Hayesep DB (30 ft × 1/8 in OD × 2 mm ID, 100/120 mesh, Stainless Steel) were used. The exit gas molar flowrates (F) was employed to compute the reactant gas conversion and product gas formation which can be represented by the following equations (5) to (8):

$$X_{CO_2}(\%) = \left[\frac{F_{CO_2}(in) - F_{CO_2}(out)}{F_{CO_2(in)}}\right] \times 100 \quad (5)$$

$$X_{CH_4}(\%) = \left[\frac{F_{CH_4}(in) - F_{CH_4}(out)}{F_{CH_4(in)}}\right] \times 100 \quad (6)$$

$$H_2 yield(\%) = \left[\frac{F_{H_2}(out)}{2F_{CH_4}(in)}\right] \times 100 \quad (7)$$

$$CO\ yield(\%) = \left[\frac{F_{CO}(out)}{F_{CH_4}(in) + F_{CO_2}(in)}\right] \times 100 \quad (8)$$

3. RESULTS AND DISCUSSION

3.1 Catalyst characterization

The elements and composition of the catalyst was determined by Energy dispersive X-ray (EDX) spectra and the results are presented in Fig. 1. The data from elemental analyses indicate that the concentration of Sm, Co and O were very close to the intended value, indicating a good preparation method.

A summary of the textural properties is represented in Table 1. The BET surface area of $SmCoO_3$ perovskite was 6.0 m^2 g^{-1}, which is an inherent property of perovskite oxides [12]. The Nitrogen adsorption-desorption isotherm for the $SmCoO_3$ perovskite catalyst represented in Fig. 1, shows a type IV adsorption isotherm similar to reported isotherms for perovskite catalyst in literature [13]. The isotherm is characteristic of mesoporous solids having pore diameter ranged 2.0-50.0 nm.

Thermogravimetric analysis of $SmCoO_3$ was carried out before calcination and the result is as shown in Fig. 3. The thermal decomposition can be represented with two peaks. The first at 473 K ascribed to water removal and partial decomposition of citric acid. It has been reported that citrate decomposition starts between 463 and 552 K [14]. The second weight loss at 560 K, attributed to destruction of the metal complex and subsequent formation of the perovskite catalyst [15].

Fig. 4 represents XRD diffractogram of fresh $SmCoO_3$ perovskite catalyst. The most intense peak at 2θ value of 33.9° indicates the formation of $SmCoO_3$ crystalline and monophasic phase. Several other peaks noticed with 2θ values of 23.9º, 26.7º, 35.8º, 41.9º, 43.6º, 48.6º, 50.2º, 54.9º, 55.9º, 60.7º, 66.9º, 71.1º, 76.3º can also be assigned to the $SmCoO_3$ crystalline species. Apart from the $SmCoO_3$ perovskite phase, no other phase was detected in the diffractogram indicative of a pure crystalline perovskite structure. The obvious peaks in the diffractogram confirm the emergence of single phase orthorhombic perovskite structure matching with JCPDS (00-025-1071). Using the Debye-Scherrer equation, the crystallize size was found to be 35.5 nm. Similar studies on the properties of $SmCoO_3$ showed crystal size of between 30 – 35 nm [16].
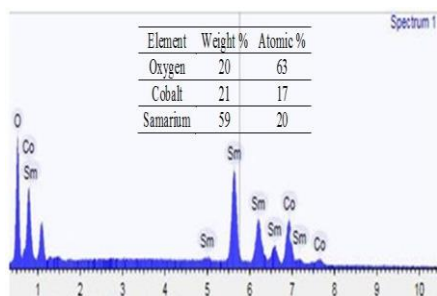

Fig. 1 EDX spectra showing the elemental composition of the fresh $SmCoO_3$ perovskite.

Table 1 Textural properties of the $SmCoO_3$ perovskite catalyst.

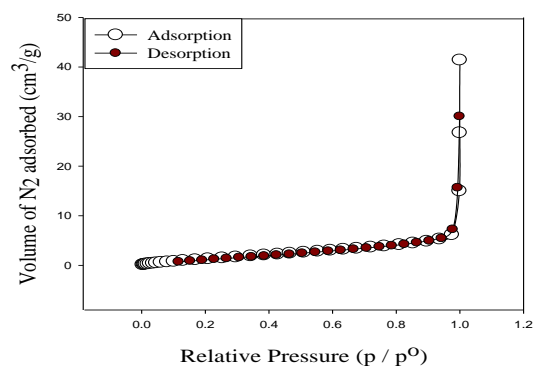| Sample	BET specific surface area (m^2 g^{-1})	Cumulative pore	
		Volume (cm^{3}g^{-1})	Diameter (nm)
$SmCoO_3$ perovskite	6.0	8.6 x 10^{-3}	6.8

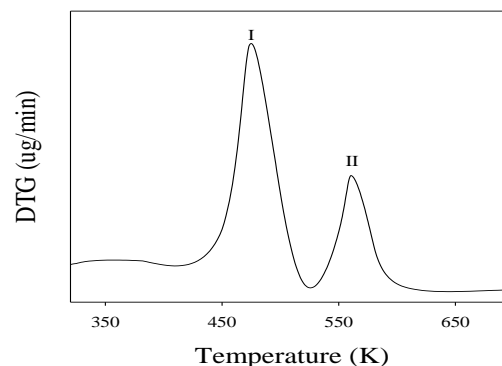**Fig. 2** N$_2$ physisorption isotherm of $SmCoO_3$ perovskite Catalyst

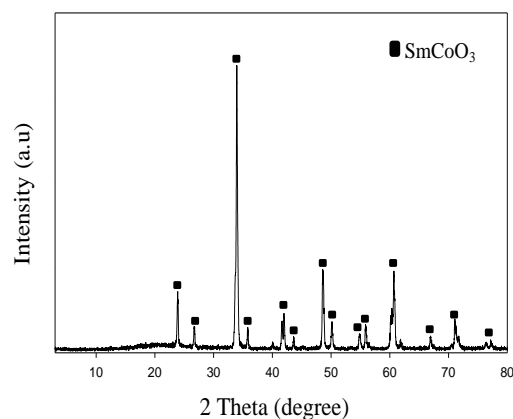**Fig. 3** Temperature programmed calcination for the uncalcined $SmCoO_3$ perovskite catalyst.

Fig. 4 X-ray diffractogram of the fresh $SmCoO_3$.

3.2   Effects of feed ratio on methane dry reforming.

3.2.1 Effects on feed conversion and product formation

The stoichiometric effects of feed ratio on methane conversion by reforming with CO_2 to yield H_2 and CO was analyzed by using three different stoichiometric feed ratio (CO_2 / CH_4) viz; 0.5, 1, 2 at temperature of 1023 K. Fig. 5a shows the activity of $SmCoO_3$ perovskite catalyst in the

methane dry reforming reaction relative to feed ratio. At feed gas ratio of 0.5 where CO_2 was the limiting reagent, methane conversion was 66 %. The relatively high conversion can be attributed to the excess supply of methane in the primary reaction (cf. Eq. 3). Highest percentage of methane conversion 84% is observed at feed gas ratio of 1.0, due to the fact that from the stoichiometry of the reaction, methane dry reforming proceed at equimolar conditions (1.0). The least methane conversion of 57% was seen at feed ratio 2.0, as a result of CH_4 being the limiting reagent in the primary reaction (cf. Eq. 3). In addition, the carbon from the decomposition of methane needs to be constantly removed by reaction with CO_2. When this process of carbon removal is delayed there is an adverse effect on the conversion of methane hence, leading to a drop in methane conversion. Researchers who also studied the effects of feed ratio on catalytic performance observed similar conversion with Ni/Al_2O_3 catalyst [17]. CO_2 conversion was highest at 0.5 feed gas ratio (89 %) and slightly dropped to 85 % at feed ratio of 1.0. upon further increase in feed ratio to 2.0, conversion of CO_2 diminished to 53% indicating that excess CO_2 does not favor the primary reaction. CO_2 is converted in the methane reforming reaction primarily by reaction with carbon; also known as the reverse Boudouard reaction; $CO_2 + C \rightarrow 2CO$.

Fig. 5b represents the production of syngas at 3 different feed ratios at 1023 K over the $SmCoO_3$ perovskite catalyst. Increase in feed ratio from 0.5 to 1.0 shows a noticeable rise in the production of H_2 from 45 to 60%. However, at excess CO_2 supply (feed ratio 2.0), the H_2 yield diminished to 32%. This trend shows that excess feed

gas supply does not favour the formation of H_2 which is similar to pattern observed for methane conversion. Production of CO over feed ratios of 0.5, 1.0, 2.0, showed similar trends to that of H_2. As feed ratio increased from 0.5 to 1.0, CO yield increased from 44 to 57 %. Further increase in feed ratio (excess CO_2) showed a drop in yield to 38 %. At excess CH_4 supply, more carbon is formed from methane decomposition leading to catalyst pores blockage [18]. Moreover, the reverse gas shift uses up produced H_2 at excess CO_2 leading to a drop in H_2 yield [19]. Similar study have been attempted in literature using lanthania-supported Co catalyst, with results showing slightly lesser activity for metal on support catalyst [20], and similar activity for perovskite-type oxides catalyst $LaRu_xNi_{1-x}O_3$ $(0.0 < x < 1.0)$ [21].

3.2.2 Effects on reaction rates

Fig. 6 shows the consumption rates of reactant gases plotted against feed ratio. Increasing feed ratio shows an increase in methane consumption rate from 7 to 9 mmol g^{-1} s^{-1}. At above stoichiometry, (feed ratio 2.0) the reactant rate diminishes to 0.4 mmol g^{-1} s^{-1} clearly showing that excess CO_2 does not favor the reaction. In contrast to methane rate, at below stoichiometry (feed ratio 0.5), consumption rate of CO_2 is 14 to mmol g^{-1} s^{-1}. This rate is seen to drop slightly to 10 mmol g^{-1} s^{-1} at stoichiometry (feed ratio 1.0) and then declines sharply at above stoichiometry (feed ratio 2.0).
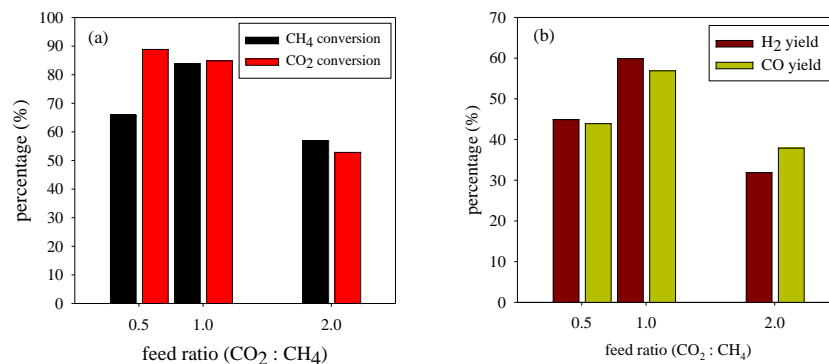

Fig. 5 Activity test for methane dry reforming over $SmCoO_3$ perovskite catalyst (a) reactants conversion (b) syngas production.

3.3 Characterization of used $SmCoO_3$ perovskite catalyst

Fig. 7 shows the Electron Dispersive X-ray spectra and the elemental composition of the used $SmCoO_3$ perovskite catalyst at stoichiometry ratio. It is evident that carbon was deposited on the catalyst surface after reaction which is characteristic of methane dry reforming reactions. In this type of reactions, methane decomposition occurs at the catalyst surface, leading to adsorbed carbon evolution. The produced carbon eventually reacts with CO_2 to produce CO in the reverse Boudouard reaction which is

favored at high temperature [22]. Accumulation of carbon in the catalyst surface leads to increase in the reactor bed volume hence, an increase in pressure gradient across the catalyst and subsequent catalyst deactivation [23].

Fig. 8 represents the temperature programmed oxidation for the used $SmCoO_3$ perovskite catalyst at stoichiometric ratio 1.0. The profile shows the derivative weight loss of the perovskite catalyst. Two obvious peaks can be seen depicting two different types of carbon species evolving from the reforming reaction. Amorphous carbon (peak I) is likely formed at temperature range 730 – 830 K. Peak II observed at about 900 K indicates another type of

carbon species. Researchers have related peaks at the temperature to graphitic/filamentous carbon [24]. Results from the TPO are in strong correlation with that of the EDX analysis reported in Fig. 7.
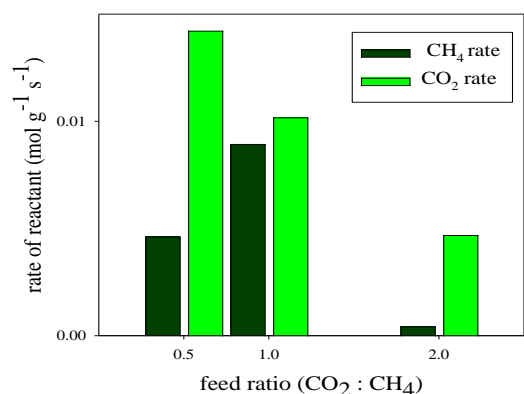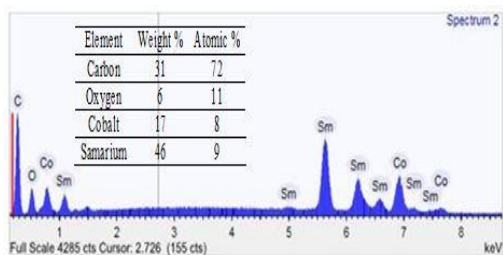

Fig. 6 Effects of feed ratio of reactants rate.

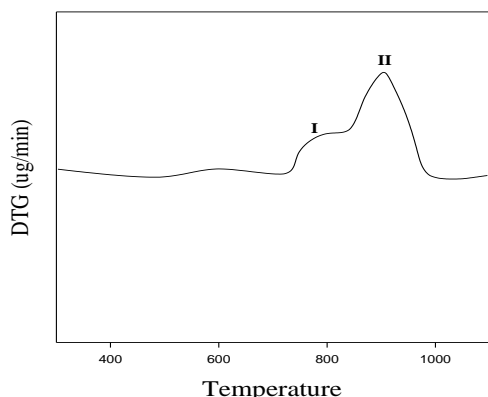**Fig. 7** EDX spectra of the used $SmCoO_3$ catalyst at feed ratio 1.0

Fig. 8 TPO profile of the used SmCoO3 perovskite catalyst at feed ratio 1.0.

4. CONCLUSION

A perovskite catalyst ($SmCoO_3$) has been synthesized by sol-gel citrate method and tested in the methane dry reforming reaction. XRD affirms the formation of crystalline and monophasic perovskite structure of the $SmCoO_3$ catalyst. The perovskite catalyst showed excellent activity for methane reforming to syngas at temperature of 1023 K, when evaluated at stoichiometry

(CO_2: CH_4 ratio 1.0), below (CO_2: CH_4 ratio 0.5), and above stoichiometry (CO_2: CH_4 ratio 2.0). The results showed that stoichiometric feed ratio affects the conversion of feed gases and the subsequent production of syngas. The optimum feed ratio for the methane reaction was seen to be 1.0. At this ratio, CO_2 and CH_4 conversion was at 85 and 84 % respectively, while H_2 and CO yield was 60 and 57 %, respectively. The results obtained verify the effectiveness of the $SmCoO_3$ perovskite catalyst in methane dry reforming reaction. In addition, used catalyst characterization from the EDX and TPO confirms two different types of carbon species formed on the catalyst surface, likely; amorphous and/or graphitic carbon species.

ACKNOWLEDGEMENTS

REFERENCES

[1] F. A. J. Al-Doghachi, U. Rashid, Y. H. Taufiq-Yap, RSC Adv. 6, (2016) 10372.
[2] E. Ruckenstein, Y. H. Hu, Appl. Catal. A Gen.. 133, (1995) 149.
[3] T. Hayakawa, S. Suzuki, J. Nakamura, T. Uchijima, S. Hamakawa, K. Suzuki, T. Shishido, and K. Takehira, Appl. Catal. A Gen. 183, (1999) 273.
[4] F. Pompeo, D. Gazzoli, N. N. Nichio, Int. J. Hydrogen Energy, 34, (2009) 2260.
[5] K. Sutthiumporn S. Kawi, Int. J. Hydrogen Energy, 36, (2011) 14435.
[6] I. V. Yentekakis, G. Goula, P. Panagiotopoulou, A. Katsoni, E. Diamadopoulos, D. Mantzavinos, A. Delimitis, Top. Catal. 58, (2015) 1228.
[7] S. Khajeh Talkhoncheh and M. Haghighi, J. Nat. Gas Sci. Eng. 23, (2015) 16.
[8] G. R. Moradi, F. Khosravian, M. Rahmanzadeh, Chinese J. Catal. 33, (2012) 797.
[9] J. K. Kim, S. S. Kim, W.-J. Kim, Mater. Lett. 59, (2005) 4006.
[10] X.-G. Zheng, S.-Y. Tan, L.-C. Dong, S.-B. Li, H.-M. Chen, S.-A. Wei, Fuel Process. Technol. 137, (2015) 250.
[11] G. S. Gallego, J. G. Marín, C. Batiot-Dupeyrat, J. Barrault, F. Mondragón, Appl. Catal. A Gen. 369, (2009) 97.
[12] E. Yang, Y. Noh, S. Ramesh, S. S. Lim, and D. J. Moon, Fuel Process. Technol. 134, (2015) 404.
[13] A. Bakandritsos, T. Steriotis, D. Petridis, Chem. Mater. 143, (2004) 1551.
[14] H. Fjellvåg, O. . Hansteen, B. . Tilset, A. Olafsen, N. Sakai, H. Seim, Thermochim. Acta. 256, (1995) 75.
[15] L. Bocher, M. H. Aguirre, R. Robert, M. Trottmann, D. Logvinovich, P. Hug, A. Weidenkaff, Thermochim. Acta. 457, (2007) 11.
[16] B. Sathyamoorthy, P. M. Md Gazzali, C. Murugesan, and G. Chandrasekaran, Mater. Res. Bull. 53, (2014) 169.
[17] Z. Alipour, M. Rezaei, F. Meshkani, J. Ind. Eng. Chem. 20, (2014) 2858.
[18] R. Pereñiguez, V. M. Gonzalez-delaCruz, A. Caballero, J. P. Holgado, Appl. Catal. B Environ. 123–124, (2012) 324.
[19] N. N. Sazonova, V. A. Sadykov, A. S. Bobin, S. A. Pokrovskaya, E. L. Gubanova, C. Mirodatos, React. Kinet. Catal. Lett.. 98, (2009) 35.
[20] B. V. Ayodele, M. R. Khan, S. S. Lam, C. K. Cheng, Int. J. Hydrogen Energy 41, (2016) 4603.
[21] G. C. de Araujo, S. M. de Lima, J. M. Assaf, M. A. Peña, J. L. G. Fierro, M. do Carmo Rangel, Catal. Today, (2008) 133.
[22] J. Dias, J. Power Sources 137, (2004) 264.

[23] V. V. Chesnokov, V. I. Zaikovskii, R. A. Buyanov, V. V. Molchanov, L. M. Plyasova, Catal. Today 24, (1995) 265.

[24] S. Wang and G. Q. M. Lu, J. Chem. Technol. Biotechnol. 595, (2000) 589.